Influence of pump wavelength and crystal length on the phase matching of optical rectification

Nick C. J. van der Valk and Paul C. M. Planken

Faculty of Applied Sciences, Delft University of Technology, Lorentzweg 1, 2628 CJ Delft, The Netherlands

Anton N. Buijserd and Huib J. Bakker

Institute for Atomic and Molecular Physics, Stichting voor Fundamenteel Onderzoek der Materie, Kruislaan 407, 1098 SJ Amsterdam, The Netherlands

Received October 19, 2004; revised manuscript received January 25, 2005; accepted February 9, 2005

We present measurements on terahertz generation by optical rectification, in which both the thickness of the generation crystal and the wavelength of the generating optical pulse are varied. The difference between the group velocity at optical frequencies and the phase velocity at terahertz frequencies affects the time trace and spectrum of the generated terahertz pulse. For the thickest crystal, we find that the phase mismatch gives rise to the generation of two pulses, separated by 4.5 ps. The physical origin of the observed features is clarified with a simple model that includes phase matching and absorption.

OCIS codes: 190.7110, 300.6270.

1. INTRODUCTION

Optical rectification is an important and frequently used method to generate broadband terahertz radiation. In this method, an ultrashort optical pulse is focused onto a crystal and radiates a terahertz pulse. The generated electric field follows the second time derivative of the optical pulse intensity. Phase matching plays an important role in the optical rectification process because the group velocity of the optical pulse will, in general, differ from the terahertz phase velocity. As a result, terahertz radiation originating from different parts of the crystal will not necessarily add up constructively.

Many experimentalists tend to avoid phase-matching issues by use of a thin generation crystal.[1,2] In a thinner crystal, a difference between the optical group velocity and the terahertz phase velocity will cause a smaller phase difference, thus limiting the amount of destructive interference. However, a thin crystal is not the best choice for each application. First, decreasing the crystal thickness results in a decrease of the emitted terahertz power. Second, terahertz radiation emitted from thin crystals will suffer strongly from Fabry–Perot reflections at the crystal interfaces. Finally, thin crystals can be very fragile, which can be a drawback in commercial applications.

For a designer of a broadband terahertz system based on optical rectification it is important to understand how the generated terahertz spectrum is affected by phase matching. There have been previous reports on this issue focusing on both theory[3,4] and experiments.[5–7] However, none of the reported experiments show how the phase-matching effects depend on the terahertz frequency, the wavelength of the generating pulse, and the thickness of the generation crystal.

We investigated the role of phase mismatch on the generated terahertz pulse shape by using generation crystals of different thicknesses. We find that changing the crystal thickness has a large effect on both the shape of the terahertz pulse and of the spectrum, which contains an oscillatory structure. Varying the pump wavelength changes the oscillation period in the spectrum, which is in excellent agreement with a theoretical model that we use to describe our measurements. These results significantly increase our understanding of the generation of terahertz radiation by optical rectification and can be used to optimize the generation process.

2. MEASUREMENT SETUP

Figure 1 shows a schematic of the measurement setup. A Ti:sapphire oscillator produces optical pulses with a duration of $\approx$100 fs, a repetition rate of 80 MHz, and a wavelength of 810 nm. The beam from this oscillator is split into two parts. The weaker part is used to detect the generated terahertz radiation, while the stronger part is used to pump an optical parametric oscillator (OPO). In the OPO, which is built around a $KTiOPO_4$ (KTP) nonlinear crystal, a parametric process converts the 810 nm Ti:sapphire pulses into pulses with a wavelength tunable between 1070 and 1240 nm and a pulse duration of $\approx$150 fs. The OPO also produces a second beam, often referred to as the idler beam, but this beam is not used in the experiments reported here.

The beam generated in the OPO goes through an optical delay stage and is then focused onto a ZnTe crystal. The focused pulses generate a polarization in the crystal that follows the envelope of the pulses (optical rectification). This induced polarization radiates a terahertz transient according to $E_{\mathrm{THz}} \sim \partial^2 P/\partial t^2$. The terahertz radiation coming out of the crystal is collimated and then focused onto a second ZnTe crystal together with the weaker split-

0740-3224/05/081714-5/$15.00

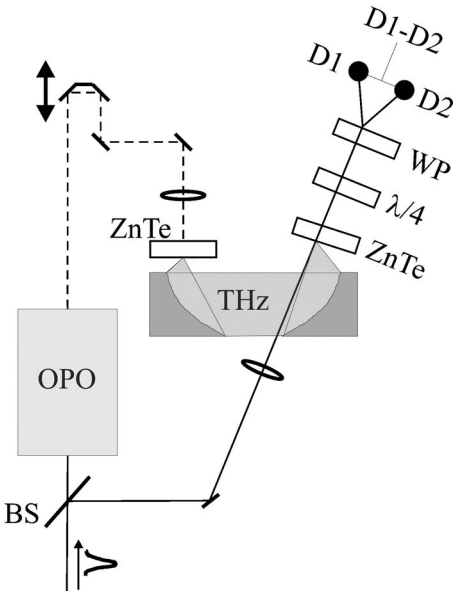

Fig. 1. Schematic diagram of the measurement setup. A beam splitter (BS) splits the Ti:sapphire beam (solid lines) into two parts. The larger part is used to pump the OPO, while the smaller part is used to detect the terahertz radiation. The beam from the OPO (dashed lines) goes through an optical delay stage and is then focused onto a ZnTe generation crystal. The generated terahertz beam is first collimated and then focused by two parabolic mirrors. In this focus the terahertz electric field is measured with a standard electro-optic detection setup, which consists of a ZnTe detection crystal, a quarter-wave plate (λ/4), a Wollaston prism (WP), and a differential photodetector.

off beam from the Ti:sapphire oscillator. In this second ZnTe crystal, which is 1 mm thick, the terahertz electric field induces a change in the polarization of the Ti:sapphire beam. This change is measured in a conventional electro-optic detection setup, leading to an electronic signal proportional to the terahertz electric field.[8]

With the above described setup, we performed two sets of measurements. In the first set, the terahertz electric field was measured in three different generation crystals with thicknesses of 0.5, 1, and 4 mm. The wavelength of the beam from the OPO is kept fixed at 1228 nm. In the second set of measurements, the thickness of the generation crystal was 1 mm, and terahertz pulses were generated with pump wavelengths of 1080, 1148, and 1228 nm.

3. RESULTS

Figures 2A–2C show the power spectra for three different thicknesses of the ZnTe generation crystal, which were calculated from the measured terahertz electric fields displayed in Figs. 2D–2F. In the calculation of the spectra, zeros were added at the end of the time traces to smooth the spectra somewhat.

The spectra show that for all three thicknesses the power is very low at low frequencies (<0.5 THz) and is zero above approximately 2.5 THz. At intermediate frequencies, the effect of phase matching becomes clearly visible in Figs. 2A–2C. The spectra show oscillations with a period that decreases as the crystal thickness increases.

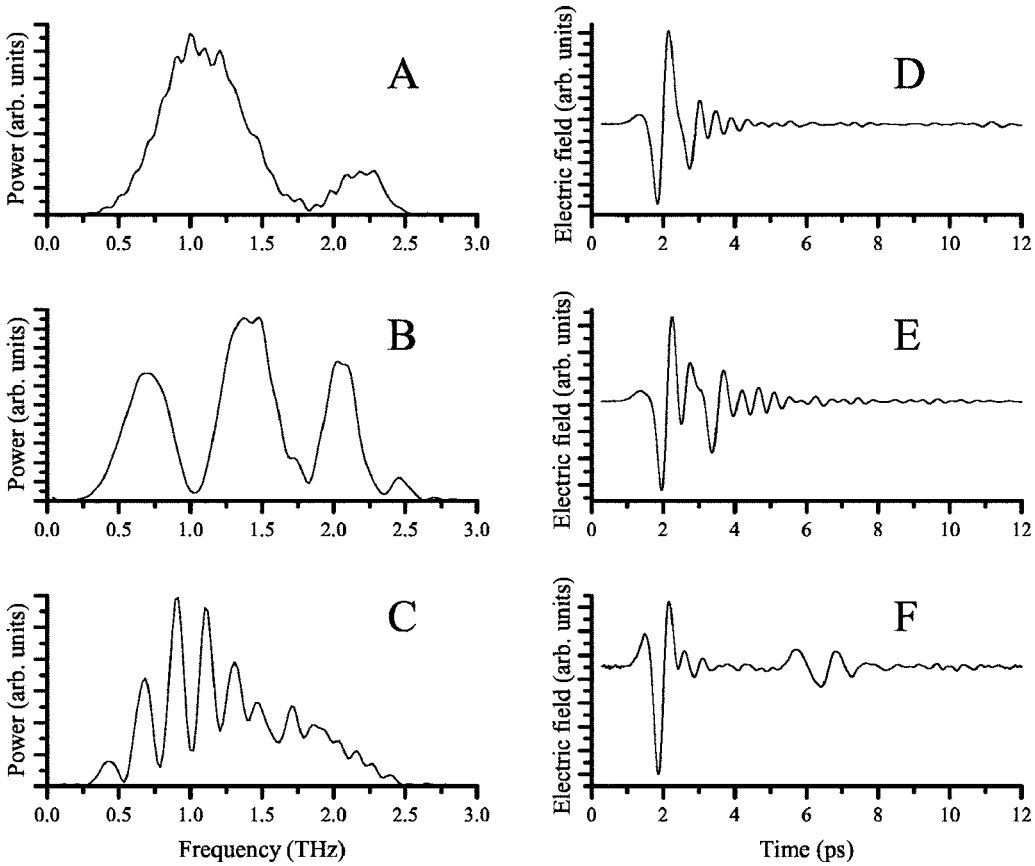

Fig. 2. Measured terahertz power spectrum with the corresponding time traces. A and D show, respectively, the spectrum and the time trace for a 0.5 mm thick generation crystal; B and E are for a 1.0 mm thick crystal; C and F are for a 4.0 mm thick crystal.

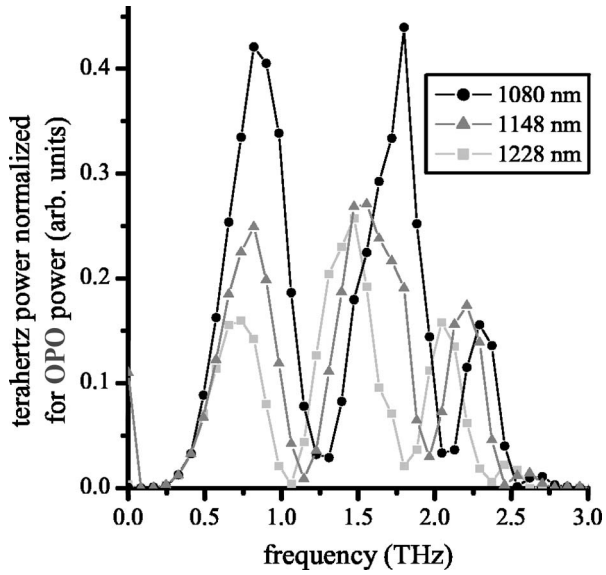

Fig. 3. Measured power spectra of terahertz radiation generated and detected in two 1 mm thick ZnTe crystals. The three spectra are generated with optical wavelengths of 1080, 1148, and 1228 nm, respectively.

The oscillations are far less pronounced in the measurement with the 4 mm thick generation crystal than in the measurements with the other two crystals. In addition, for the 4 mm crystal the oscillations strongly decrease in amplitude above 1.5 THz.

Further insight in the origin of the oscillations shown in Figs. 2A–2C is obtained by looking at Fig. 2F. Remarkably, this measurement shows that the terahertz signal consists of two pulses separated by ≈4.5 ps. These pulses are not identically shaped; the second pulse is smaller and clearly contains fewer high-frequency components. Reflections in the generation crystal and the detection crystal have a delay of 78 and 21 ps, respectively, and thus cannot explain the pulses observed in Fig. 2F.

Figure 3 shows results from the second set of measurements in which we measured the terahertz radiation generated in a 1 mm thick ZnTe crystal for three different wavelengths of the generation beam, 1080, 1148, and 1228 nm. The measured electric fields were divided by the power delivered by the OPO at each wavelength to enable a quantitative comparison of the terahertz powers generated at different pump wavelengths. For all three wavelengths, the spectra in Fig. 3 show strong oscillations. The period of the oscillations increases as the wavelength of the generating beam is decreased. We also observe that the amplitude of the oscillations increases with decreasing wavelength.

4. MODEL

The results of Section 3 can be described with a simple model that includes phase-matching effects in both the generation crystal and the detection crystal and absorption of terahertz radiation in the generation crystal. We disregard various, less important effects, such as absorption of terahertz radiation in the detection crystal, phase matching in off-axis directions, reflections at the crystal surfaces, and dispersion acting on the generation beam, as it can be shown that these only produce small corrections.

From Shen[9] we derive an expression for the spectrum of the terahertz electric field radiated by optical rectification:

$$E_{T\mathrm{rad}}(\omega_T) \sim \omega_T^2 \frac{1-\exp(-\alpha l_g - i\Delta k_g l_g)}{\alpha + i\Delta k_g}, \tag{1}$$

where l_g is the thickness of the generation crystal, ω_T is the terahertz radial frequency, and α is the terahertz absorption coefficient. The phase mismatch in the generation crystal Δk_g is given by $[\omega_T(\partial k_g/\partial\omega)-k_T]$, where k_T is the wave number of the terahertz beam and k_g is the wave number of the generating beam. Expression (1) does not contain a term representing the limited range of ω_T that can be generated from the pump pulse. This is valid as long as the terahertz wavelength is larger than the inverse pump pulse length.

The fraction in expression (1) can be viewed as the sum of two terms that correspond to the contributions from the front and the back of the crystal. The term $1/(\alpha+i\Delta k_g)$ can be regarded as the contribution from a part of the crystal near the back face with a length of the order of $|\alpha+i\Delta k_g|^{-1}$. The second term corresponds to a contribution from a part with a similar length near the front of the crystal. This contribution is subject to absorption in the crystal $[\exp(-\alpha l_g)]$ and gets an additional phase due to the phase mismatch $[\exp(-i\Delta k_g l_g)]$. The additional phase $\Delta k_g l_g$ is, neglecting dispersion, linear with the terahertz frequency. A linearly increasing phase in the frequency domain corresponds to a delay in the time domain. The contribution to the electric field of the second term will thus give rise to a second pulse, delayed in time with respect to the contribution of the first term. However, for small delays the two contributions will (partly) overlap in time, will interfere, and will form one pulse. Note that in the limit of thin crystals ($|\alpha l_g + i\Delta k_g l_g| \ll 1$), expression (1) becomes $E_{T\mathrm{rad}} \sim \omega_T^2 l_g$.

As can be found in the literature,[10–12] phase matching in the detection crystal leads to multiplication of the incident field with $\sin(\frac{1}{2}\Delta k_d l_d)/(\frac{1}{2}\Delta k_d l_d)$, where l_d is the length of the detection crystal and Δk_d is the phase mismatch in the detection crystal. Using this factor and expression (1) we find that the detected terahertz electric field spectrum is proportional to

$$E_{T\mathrm{det}}(\omega_T) \sim \omega_T^2 \frac{1-\exp(-\alpha l_g - i\Delta k_g l_g)}{\alpha + i\Delta k_g} \frac{\sin\left(\frac{1}{2}\Delta k_d l_d\right)}{\frac{1}{2}\Delta k_d l_d}. \tag{2}$$

Expression (2) is a strong function of the frequency of the emitted terahertz radiation since α, Δk_g, and Δk_d depend on the terahertz frequency ω_T.

5. DISCUSSION

An important aspect of the measurements is the oscillations visible in Figs. 2A–2C. These oscillations are due to

phase matching in the generation crystal. The mismatch between the group velocity of the generating pulse and the terahertz phase velocity determines the amount of destructive interference between the terahertz electric fields generated on different positions of the crystal. This phase mismatch is a strong function of the terahertz frequency, which in nondispersive media causes oscillations in the spectrum with a fixed period. However, the ZnTe crystal is dispersive, leading to variations in the period of the oscillation, which are most clear in Fig. 2B.

For thick crystals, contributions to the terahertz electric field from the center region of the crystal cancel. The 4 mm generation crystal is so thick that the remaining contributions from the crystal regions near the front and the back face are well separated in time, as can be seen in Fig. 2F. Hence, in this limit, the generated terahertz field consists of two well-separated peaks. This limiting shape of the generated terahertz field has been observed before in a study on optical rectification in $LiNbO_3$ and $LiTaO_3$ crystals.[7] The velocity of the terahertz pulse is lower than that of the generating pulse, so that the contribution from the back of the crystal arrives before the contribution from the front.

To explain the periodic feature in the measured spectra, we point out that two equally shaped pulses in the time domain give rise to an oscillation in the frequency domain. This remains true if the separation between the two pulses is such that the pulses (partly) overlap. In Fig. 2 this leads to clear oscillations in the spectra, even for the 0.5 mm thick crystal, where the pulses are barely separated.

The two peaks in Fig. 2F are not equally shaped; the pulse from the front of the crystal is smaller and contains fewer high-frequency components. This decreases the modulation depth of the oscillations that can be seen in Fig 2C. The main reason for the different shapes of the two pulses in Fig. 2F is that the pulse generated at the front of the crystal has to travel all the way through the ZnTe crystal and is thus strongly subject to absorption and dispersion. The power absorption coefficient of ZnTe rises from 2 cm^{-1} at 1 THz to 13 cm^{-1} at 1.6 THz,[13] which cannot be neglected for a 4 mm thick crystal. In addition, the focal length of the generating beam is smaller than the length of the crystal, which implies, in this case, that the diameter of the generating beam is larger at the front of the crystal than it is at the back. This leads to a reduced radiation efficiency at the front, and thus to less pronounced oscillations.

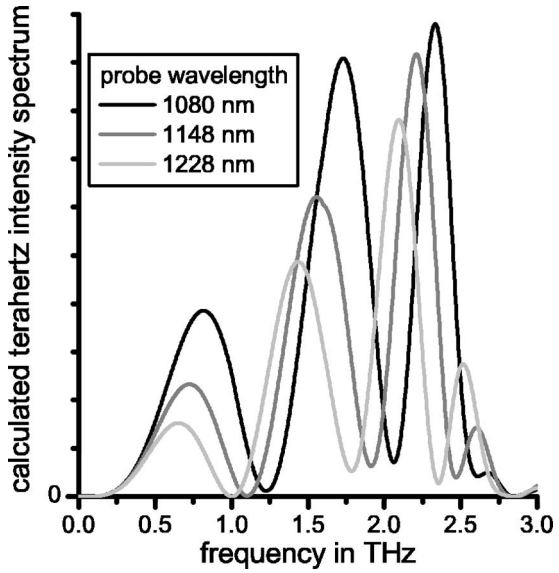

Fig. 4. Terahertz intensity spectra calculated with expression (2). Three spectra are shown, corresponding to three different wavelengths for the optical beam used to generated the terahertz radiation.

We now consider how the radiated terahertz spectrum depends on the wavelength of the generation pulse. As can be seen in Fig. 3, the period of the oscillations in the spectrum increases as the wavelength of the generation beam decreases. As this wavelength decreases, the phase mismatch in the terahertz generation process becomes smaller, and the minima of the oscillations shift toward higher terahertz frequencies.

Figure 4 shows the terahertz intensity spectrum for the generation beam wavelengths of 1080, 1148, and 1228 nm used in the experiments, calculated with expression (2). For the refractive indices of ZnTe at optical and terahertz frequencies, we used, respectively, Refs. 14 and 15. The terahertz absorption coefficient α is obtained from Ref. 13. In the calculation, l_d and l_g are both 1 mm and the wavelength of the detection beam is 810 nm.

Comparing Fig. 4 with Fig. 3, we find that the model accurately predicts the minima of the oscillations in the measured spectra. Closer examination shows that the largest distance between the measured and the calculated minima is 62 GHz. This is an excellent agreement, considering the expected uncertainty in the values of the refractive indices.

The values of the oscillation minima in Fig. 3 do not reach zero intensity around 2 THz, which contrasts with the results around 1 THz. This feature of our measurement is also in good agreement with the calculated results of Fig. 4. Absorption weakens the contributions from the front of the crystal more than the contributions from the back, since the contribution from the front region has to travel longer through the crystal. This means that destructive interference between the front and the back region cannot be complete.

We conclude the discussion of the spectrum of the emitted terahertz radiation by considering the low- and high-frequency edges of the spectrum. From Figs. 2A–2C it can be seen that at low frequencies the power decreases to zero. This is due to the conversion from the nonlinearly induced polarization in the crystal to far-field radiation, since the radiated electric field of any polarization is proportional to the second time derivative of the polarization ($E_{\mathrm{THz}} \sim \partial^2 P / \partial t^2$). A second time derivative corresponds to a factor $-\omega_T^2$ in the frequency domain, where ω_T is the terahertz radial frequency. The radiation efficiency at low frequencies, where phase-matching effects are still negligible, is thus proportional to ω_T^2.

The lack of spectral content roughly above 2.5 THz in Figs. 2A–2C is partly due to phase matching in the detection crystal as is confirmed in our calculations in Fig. 4. We emphasize that the detection process, which uses an 810 nm beam, is much better phase matched than the generation process. We calculated that the detection effi-

ciency should decrease with frequency due to phase matching in the detection crystal, until the detection efficiency reaches zero at 2.8 THz. The detected signal suffers from additional frequency-dependent decreases due to absorption in the detection crystal and due to the nonzero pulse length of both the detection and the generation optical pulses. These effects are not included in our model, which explains the difference between measurement and calculation of the oscillation amplitudes at high frequencies.

6. CONCLUSION

We have presented measurements and calculations that show how the spectrum of a terahertz pulse generated by optical rectification depends on the thickness of the generation crystal and on the wavelength of the optical generation pulse. The measured spectra have strong oscillations, which are caused by constructive and destructive interference between contributions to the radiated field from different parts of the crystal. This phase-matching effect is strongly dependent on the thickness of the crystal. In the measurement with a 4 mm thick crystal, all contributions to the radiated field from the central region of the crystal cancel out and only the contributions from regions near the two faces of the crystal survive, leading to the formation of two terahertz pulses, separated in time.

The measured spectra depend on the wavelength of the generation beam, because this wavelength determines the phase mismatch. We present a model that is accurate enough to describe the main features of the measured spectra.

ACKNOWLEDGMENT

This work was performed as part of the research program of the Stichting voor Fundamenteel Onderzoek der Materie, which is financially supported by the Nederlandse Organisation voor Wetenschappelijk Onderzoek.

The e-mail address for N. C. J. van der Valk is n.c.j.vandervalk@tnw.tudelft.nl.

REFERENCES

1. R. Huber, A. Brodschelm, F. Tauser, and A. Leitenstorfer, "Generation and field-resolved detection of femtosecond electromagnetic pulses up to 41 THz," Appl. Phys. Lett. **76**, 3191–3193 (2000).
2. K. Liu, J. Xu, and X.-C. Zhang, "GaSe crystals for broadband terahertz wave detection," Appl. Phys. Lett. **85**, 863–865 (2004).
3. J. R. Morris and Y. R. Shen, "Far-infrared generation by picosecond pulses in electro-optical materials," Opt. Commun. **3**, 81–84 (1971).
4. D. A. Kleinman and D. H. Auston, "Theory of electrooptic shock radiation in nonlinear optical media," IEEE J. Quantum Electron. **QE-20**, 964–970 (1984).
5. K. H. Yang, P. L. Richards, and Y. R. Shen, "Generation of far-infrared radiation by picosecond light pulses in $LiNbO_3$," Appl. Phys. Lett. **19**, 320–323 (1971).
6. A. Nahata, A. S. Weling, and T. R. Heinz, "A wideband coherent terahertz spectroscopy system using optical rectification and electro-optic sampling," Appl. Phys. Lett. **69**, 2321–2323 (1996).
7. L. Xu, X.-C. Zhang, and D. H. Auston, "Terahertz beam generation by femtosecond optical pulses in electro-optic materials," Appl. Phys. Lett. **61**, 1784–1786 (2000).
8. P. Uhd Jepsen, C. Winnewisser, M. Schall, W. Schyja, S. R. Keiding, and H. Helm, "Detection of THz pulses by phase retardation in lithium tantalate," Phys. Rev. E **53**, R3052–R3054 (1996).
9. Y. R. Shen, "Far-infrared generation by optical mixing," Prog. Quantum Electron. **4**, 207–232 (1976).
10. H. J. Bakker, G. C. Cho, H. Kurz, Q. Wu, and X.-C. Zhang, "Distortion of terahertz pulses in electro-optic sampling," J. Opt. Soc. Am. B **15**, 1795–1801 (1998).
11. G. Gallot and D. Grischkowsky, "Electro-optic detection of terahertz radiation," J. Opt. Soc. Am. B **16**, 1204–1212 (1999).
12. M. Schall and P. Uhd Jepsen, "Freeze-out of difference-phonon modes in ZnTe and its application in detection of THz pulses," Appl. Phys. Lett. **77**, 2801–2803 (2000).
13. G. Gallot, J. Zhang, R. W. McGowan, T.-I. Jeon, and D. Grischkowsky, "Measurements of the THz absorption and dispersion of ZnTe and their relevance to the electro-optic detection of THz radiation," Appl. Phys. Lett. **74**, 3450–3452 (1999).
14. D. T. F. Marple, "Refractive index of ZnSe, ZnTe, and CdTe," J. Appl. Phys. **35**, 539–542 (1964).
15. A. Manabe, A. Mitsuishi, and H. Yoshinaga, "Infrared lattice reflection spectra of II-VI compounds," Jpn. J. Appl. Phys. **6**, 593–600 (1967).